



## A computational Method for Bilateral Symmetry Recognition in Asymmetrically Scanned Human Faces

Luca Di Angelo<sup>1</sup> and Paolo Di Stefano<sup>2</sup>

<sup>1</sup>University of L'Aquila, [luca.diangelo@univaq.it](mailto:luca.diangelo@univaq.it)

<sup>2</sup>University of L'Aquila, [paolo.distefano@univaq.it](mailto:paolo.distefano@univaq.it)

### ABSTRACT

This paper presents a new mirroring-and-registration method for the automatic symmetry plane detection of 3D asymmetrically scanned human faces. Once the mirroring of the original data is carried out with respect to the first-attempt symmetry plane, which is estimated by the *PCA* method, the source point cloud and the mirrored data are registered by the ICP algorithm that minimises a new weighted function. The final symmetry plane obtained approximates in the least-squares sense the midpoints of the lines connecting homologous points randomly chosen. This method is validated by analysing some specifically-designed test cases. The obtained results show that the method is quite insensitive to asymmetries of data resulting from the acquisition process.

**Keywords:** symmetry plane, iterative closest points, rasterstereography, registration, mirroring

### 1. INTRODUCTION

One of the most important geometric features of the human face is the plane identifying its bilateral symmetry. Thanks to the possibility of having 3D data of the face, the bilateral *symmetry plane* can be recognized and evaluated by means of properly processed face data. The knowledge of the *symmetry plane* could be useful for various purposes, such as:

- face authentication ([13] and [21]);
- face reconstruction or cosmetic surgery for aesthetic corrections in Maxillofacial Surgery ([1], [9]);
- facial asymmetry and symmetry line correlation for back pathologies in Orthopaedics and Orthodontics [11];
- facial symmetry and cognitive disorders correlations for schizophrenia diagnosis in Neurology [10].

In many practical cases the data relating to an acquired human face are incomplete and not symmetrically acquired. These limitations are mainly due to the typical technologies used in 3D geometric scanning. These technologies require that each and every part of the face should be completely visible from the device viewpoint. Considering the anatomy of the face, many parts may result in undercut and therefore may not be acquired. The portion of the face which can actually be scanned depends on the face's

distance from and orientation with respect to the scanning device. In real cases bilateral symmetry must be recognized on a partially acquired surface, which is also affected by a non-uniform point density. Thus the information which attempts to recognise human face symmetry must be extracted from an asymmetric point cloud. Other factors which may blur the symmetry recognition process can be identified in some physiognomic asymmetries of the human face, such as local damage, pimples, bumps, wrinkles, etc. Typically, the methods presented in literature are conceived and tested to analyse cases where the face is completely acquired. They fall short in the case of asymmetrically scanned data and whenever there is a non-uniform sampling density. With a view to detecting the *symmetry plane* of asymmetrically scanned human faces, this paper presents a new method. Its performance, in terms of robustness and accuracy, is quantified as to the *symmetry plane* detection of some real test cases.

### 2. RELATED WORKS

The methods for human face *symmetry plane* detection can be classified under the following two categories:

- Extended Gaussian Image (EGI),
- mirroring and registration.



The Extended Gaussian Image of a polyhedron is a special kind of Gaussian map in which the normal direction of planar triangular facets is weighted by the extension area. The *EGI* methods analyse the symmetry of the *EGI* map and are based on the practical observation according to which in many cases if an object is symmetric, then so is the *EGI* [18]. The first approach for the determination of the *symmetry plane* of objects, based on *EGI*, is proposed by Sun and Sherrah in [18]. They analyse the recurrence histogram of the orientation of the normal unit vectors from *EGI* and, in order to reduce the computational costs, the *EGI* map is examined only around the principal axes of inertia of the orientation histogram. With the intent to increase the robustness of the method in the presence of noisy data, Pan et al. in [12] compute the orientation histogram by the inverse of the Gaussian curvature. The method's robustness is improved by evaluating the Gaussian curvature by paraboloid fitting, which estimates the differential geometric properties by making an average on a larger neighbourhood than that explored by discrete methods [19]. The *EGI*-based methods do not perform the analysis of the symmetry of the geometry but the results they yield are conditioned by the symmetry of the acquisition.

The mirroring-and-registration methods perform the *symmetry plane* detection directly by verifying the possibility of superimposing the point cloud with its mirroring. Typically, these methods carry out an initial rough estimation of the *symmetry plane* ( $\Pi_0$ ). Then the mirroring ( $PC_m$ ) of the original data ( $PC$ ) is performed with respect to  $\Pi_0$ . The  $PC$  and  $PC_m$  are registered by the *Iterative Closest Point* algorithm (*ICP* [3]), obtaining  $PC_{m,r}$ . The final estimation of the *symmetry plane*  $\Pi_f$  is evaluated by approximating, in the least-squares sense, the middle points of the segments joining homologous points in  $PC$  and  $PC_{m,r}$ .

M. Benz et al. [1] were the first to propose the mirroring-and-registration method in order to support aesthetic surgical facial reconstruction. Their work aims at the detection of the *symmetry plane* by means of which the healthy half can be mirrored onto the damaged half for its reconstruction. The authors highlight how the choice of typically healthy areas in a damaged face (nose, chin and forehead) turns out to be sufficient to register the original data and the mirrored data through a specific *ICP* algorithm [16].

A variant of the typical approach is proposed by De Momi et al. in [9], which performs the first-attempt estimation of the *symmetry plane* as the *symmetry plane* of the centroids of manually selected areas.

In order to develop a fully automatic method, Colbry and Stockman in [5] put forward an approach whereby the first-attempt *symmetry plane* is evaluated by the *Principal Component Analysis* (*PCA*) method [14]. As highlighted by Tang et al. in [20], this approach could fail with asymmetrically scanned

data. In those cases the *PCA* method performs so inaccurate an estimation of the *symmetry plane* that the subsequent *ICP* registration algorithm could not converge. In order to overcome this limitation, the authors in [20] propose the plane being parallel to the  $yz$  - plane and passing through the centroid of the face for an initial estimate. This approach works correctly only if the real *symmetry plane* is aligned with the  $yz$  - plane of the scanning device. In order to perform an *ICP* registration which is insensitive to asymmetrical data, Tang et al. in [20] focalize the registration by analysing a rectangular region symmetrically selected around the nose. It is a valid approach only in the case of undistorted noses.

Zhang et al. in [21] point out that the *ICP* algorithm could fail when there are irregularities in the face boundary. Therefore, in their paper, the authors propose the *MarkSkirt* operator which excludes from the registration the points belonging to the 10-ring of the boundary.

More recently, Combès et al. in [7], [6] and [8] present an approach that directly estimates the *symmetry plane* without intermediate roto-translation transformation and registration. Once the initial estimation of the *symmetry plane* is performed by the *PCA* method, its final evaluation  $\Pi_f$  is done by an iterative algorithm that converges to a (at least local) minimum of a properly designed function. In particular, this function is the sum of the weighted distances between the points reflected with respect to  $\Pi_f$  and the corresponding nearest points of the cloud. With a view to leaving out the asymmetric sampled area of the model, weights are expressed as the *Leclerc function* [4]. The problem of the non-symmetrical sampling of the face is solved by this method but it is still sensitive to non-uniformity in the sampling. Two homologous surfaces which are perfectly symmetric but which are characterized by different sampling density may turn out to be asymmetric due to the distance between the source point cloud and the mirrored - registered one.

*ICP* algorithms are the main cause for a rise in computational costs so great efforts have been directed towards speeding up this algorithm in [1], [7] and [6]. Spreeuwers in [17], proposes a mirroring and registration method that is not based on the *ICP*. The estimation of the *symmetry plane* is found by varying the value of the parameters identifying it ( $\vartheta$ : rotation around the  $y$ -axis;  $\varphi$ : rotation around the  $z$ -axis;  $d_x$ : the  $x$  coordinate of the intersection of the *symmetry plane* with the  $x$ -axis) in a range and with steps value defined by the user. The solution is that for which the distance between the corresponding points of the cloud and the mirrored one is minimum. This method is computationally more efficient of the *ICP* but it doesn't solve the critical aspects previously evidenced.

### 3. THE PROPOSED METHOD

In general, any geometric form  $S$  in three dimensions is said to be *bilaterally symmetric* with respect to  $\Pi$  if its mirror image ( $S_{\Pi}$ ) upon  $\Pi$  is partially or completely superimposable onto the original form and the plane  $\Pi$  is the *symmetry plane* of  $S$ . Perfect symmetry is an ideal condition that is not verified in any real object, let alone in the case of human faces. Furthermore, no method for the *symmetry plane* estimation of a geometric facial feature can verify the previous symmetry definition. Therefore, for any real symmetrical object, symmetry can be recognized as a property of a non-ideal shape which is not very far from an ideally perfect, bilaterally symmetric shape.

Also in the case of an object which is defined discretely by a set of points pertaining to its surface, the symmetry property should refer to its shape and not to the point cloud itself. Asymmetry pertaining completely to the point cloud and, not to the shape, can be due to surface density sampling or to the asymmetry of the acquired area.

In a typically 3D surface scanning process, the density of point sampling depends on the surface orientation with respect to the observation direction. Surfaces oriented orthogonally to the view direction are sampled more densely than those in foreshortened views. The density of point sampling, depending on the orientation of the face with respect to the scanner, is not symmetrically mapped.

The asymmetry in the acquired area depends on many factors. Due to the orientation of the face with respect to the observation view, those parts of the face which remain hidden are not acquired (an example is reported in figure 1a). Another factor is irregularities in the borders of the acquired surface which can be due to hairline, shaving or the direction of the viewpoint, which does not pertain to the *symmetry plane*. Such is the case shown in figure 1b.

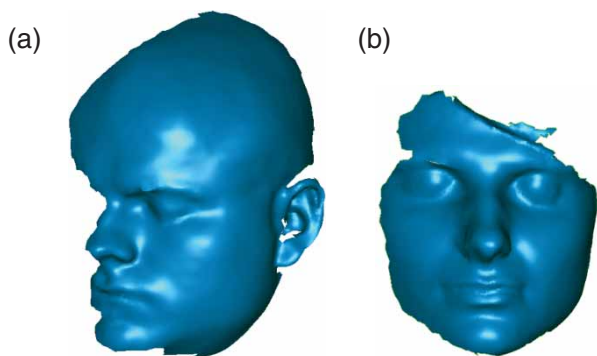


Fig. 1: Examples of asymmetrically scanned data.

Finally, the evaluation of the *symmetry plane* of a human face can be affected by asymmetric facial expressions and/or by isolated local particularities, such as local damage, pimples, bumps, etc. Although these local particularities do not modify the general

symmetrical nature of the face, they could affect the automatic estimation of the symmetry plane.

The proposed method is therefore designed to overcome the above-mentioned limitations. It is based on the typical mirroring-and-registration approach, properly improved to perform a robust evaluation of the bilateral facial symmetry. The most important steps of the method are detailed in the following sections.

#### 3.1. Face Scanning

The *face scanning* step is performed by means of a 3D optical geometric scanner [1] which makes it possible to acquire, in a single scanning session, about 50,000 points with a density sampling of about 0.75 mm. In many practical applications the face is required to be acquired in just one pose; the complete reconstruction of the face geometry is not possible since more than one scanning session would be needed as well as the registration of the related point cloud. This single acquisition can be performed from a point of view which cannot ensure a symmetric scanning of the face.

Considering the typical noise affecting point cloud acquisition, the data is first smoothed by a Gaussian filter and then tessellated. Tessellation serves both to reconstruct the surface of the acquired face and to better identify frequent outliers resulting from hairs or powder in air.

#### 3.2. First-attempt Estimation of the Symmetry Plane

The quality of the first-attempt estimation of the *symmetry plane* ( $\Pi_0$ ) greatly affects the traditional approaches to the ICP registration process. This phase is so critical that it is also used to characterize and to name the methods presented in literature. In the method here proposed, the first-attempt estimation of the *symmetry plane* is performed by the *Principal Component Analysis (PCA)* [14]. This is the typical approach used to carry out a first attempt at estimating the *symmetry plane*. It evaluates the *symmetry plane* by calculating the principal inertial directions of the point cloud to be analysed. For this reason, this first attempt is more properly the *symmetry plane* of the point cloud and is therefore more affected by its extension than by the shape of the acquired surface. Nevertheless, even if this first evaluation of the *symmetry plane* is not accurate, it does not compromise the best solution offered by the next phases of the method here presented.

#### 3.3. Final Estimation of the Symmetry Plane

Starting from  $\Pi_0$ , the final estimation of the *symmetry plane* ( $\Pi_f$ ) is obtained by the refinement algorithm flowcharted in figure 2.

In each cycle the method searches for the *symmetry plane* by performing the mirroring of the original

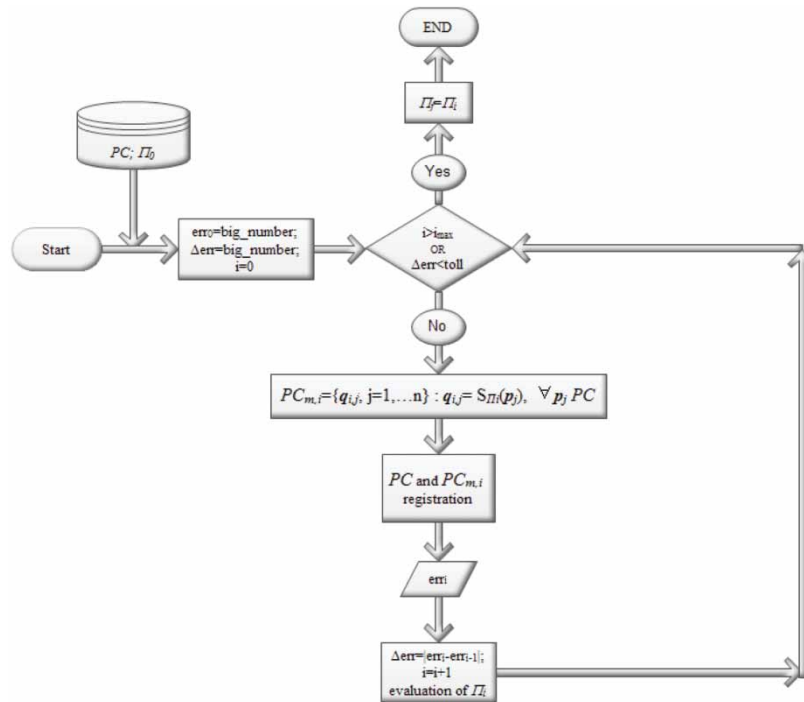


Fig. 2: Flow-chart of the proposed refinement method.

data  $PC$  with respect to the last estimation of the *symmetry plane* ( $\Pi_i$ ):

$$PC_{m,i} = \{q_{i,j}, j = 1, \dots, n\} : q_{i,j} = S_{\Pi}(p_j), \forall p_j \in PC$$

Then the source point cloud ( $PC$ ) and the mirrored data ( $PC_{m,i}$ ) are registered by a weighted *ICP* algorithm. The optimal solution is obtained by minimizing the *Hausdorff distance* properly weighed. The optimization function is as follows:

$$\frac{\sum_{j=1}^n [w_{i,j} \cdot Haus(p_j, TS(PC_{m,i}))]}{\sum_{j=1}^n w_{i,j}} \quad (3.1)$$

where:

- $n$  is the number of points of  $PC$ ;
- $p_j$  is the  $j$ -th point belonging to  $PC$ ;
- $TS(PC_{m,i})$  is the tessellated surface relative to point cloud  $PC_{m,i}$ ;
- $Haus(p_j, TS(PC_{m,i}))$  is the *Hausdorff distance* between  $p_j$  and the tessellated surface  $TS(PC_{m,i})$  according to the following equation:

$$Haus(p_j, TS(PC_{m,i})) = \min_{q_{i,j} \in TS(PC_{m,i})} \|q_{i,j} - p_j\|_2 \quad (3.2)$$

- $w_{i,j}$  are the weights.

Typically, the *Hausdorff distance* is evaluated point by point [7]; however, and due to the asymmetry in surface sampling, it is improbable for a point  $p_j$  of

$PC$  to find a point  $q_j$  of  $PC_{m,i}$  which is perfectly symmetrically located, although it can be found at a distance which largely depends on the sampling density. In this work, in order to solve the problems arising from asymmetries in surface sampling, the *Hausdorff distance* is calculated between the point  $p_j$  and the tessellated surface ( $TS(PC_{m,i})$ ). In this way the *ICP* algorithm is not affected by non-uniformity in sampling density.

The weights  $w_{i,j}$  play an important role in the functionalities of the method being presented. It is expressed as the product of two specific weights:

$$w_{i,j} = w_{s,i,j} \cdot w_{r,i,j} \quad (3.3)$$

The asymmetries in the acquisition process are mainly located far from the *symmetry plane* (figure 1a). The weight  $w_{s,i,j}$  is introduced to reduce the effect that the points far from the *symmetry plane* may have on the registration process.  $w_{s,i,j}$  is expressed according to the *Leclerc function* which has its maximum in correspondence to the *symmetry plane*:

$$w_{s,i,j} = \frac{1}{\sigma_s^2} \cdot e^{-\left(\frac{d_{i,j}}{\sigma_s}\right)^2} \quad (3.4)$$

$d_{i,j}$  is the distance between  $p_j$  and the *symmetry plane*  $\Pi_i$  and  $\sigma_s$  is the width of the window extended across the *symmetry plane*.

The weight  $w_{r,i,j}$  works as a filter which excludes from the registration process any local asymmetries,

whether they be near or far from the symmetry plane. It is defined according to the *Leclerc function*:

$$w_{r,i,j} = \frac{1}{\sigma_r^2} \cdot e^{-\left(\frac{r_{i,j}}{\sigma_r}\right)^2} \quad (3.5)$$

where  $r_{i,j}$  is the *Hausdorff distance* between  $\mathbf{p}_j$  and  $TS(PC_{m,i})$  and  $\sigma_r$  defines the radius of the analysis window whose centre is located symmetrically to  $\mathbf{p}_j$ .

Large values of  $\sigma_r$  and  $\sigma_s$  are useful in the initial phase of the iterative process when the point clouds are unregistered, whereas small values afford a greatly accurate registration of the symmetric parts

excluding local and peripheral asymmetries. In the experiments described hereafter, the values of  $\sigma_s$  and  $\sigma_r$  are first assumed to be the 100 per cent and then, in the refinement steps, the 5 per cent of the maximal width of the face.

After surface registration is complete, the *symmetry plane*  $\Pi_{i+1}$  is evaluated by randomly choosing 10,000 points of  $PC$  and the corresponding ones from the mirrored-registered point cloud ( $PC_{m,i,r}$ ). For each pair of corresponding points ( $\mathbf{p}_j, \mathbf{q}_{i,j}$ ) the middle point  $\mathbf{m}_{i,j} = \frac{\mathbf{p}_j + \mathbf{q}_{i,j}}{2}$  is calculated. Finally,  $\Pi_{i+1}$  is calculated by approximating, in the least-squares sense, all the  $\mathbf{m}_{i,j}$  points.

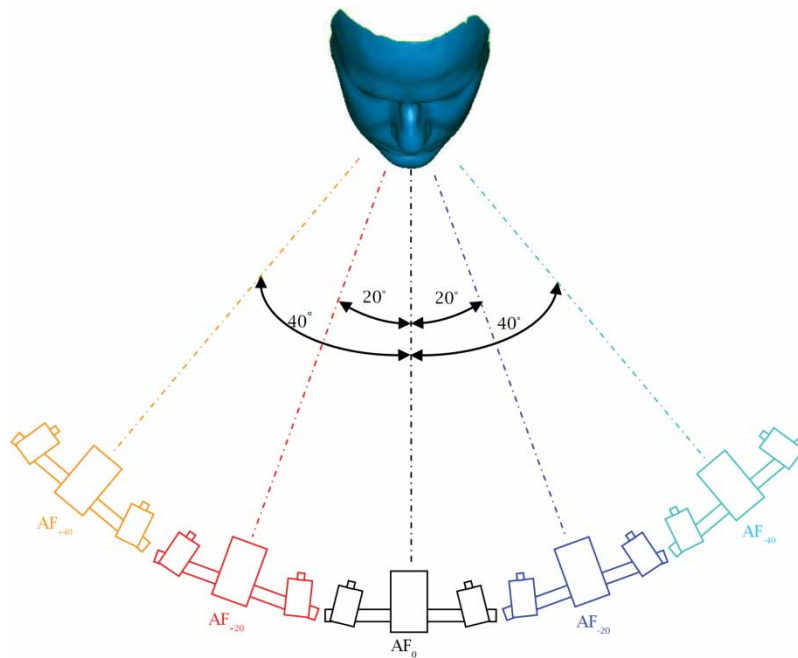


Fig. 3: Schematic representation (not to scale) and labels of the different positions assumed by the optical scanner with respect to the subject's face.

Subject label	RF	AF <sub>+40</sub>	AF <sub>+20</sub>	AF <sub>0</sub>	AF <sub>-20</sub>	AF <sub>-40</sub>
1						
9						

Fig. 4: Two of the 15 test cases here considered.

The iterative process comes to an end when the variation of function (3.1) between two iteration cycles is lower than the imposed threshold value or when the number of iterations is equal to the maximum admissible value; in both cases  $\Pi_f$  is assumed to be  $\Pi_{i+1}$ .

#### 4. EXPERIMENTS AND RESULTS

The method being proposed, henceforth labelled as *AQ method*, has been implemented in original software, coded in MATLAB. In order to have a quantitative evaluation of the *AQ method*, its performance is compared with that of our implementation of the method proposed by Pan and Wu in [13] (in what follows, the *Pan and Wu method*). All the tests have been run on a WorkStation with 3.0 GHz Intel Xeon processor and 16.0 Gb RAM.

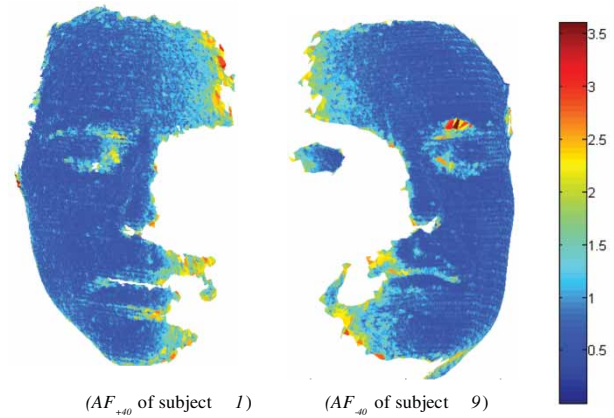


Fig. 5: Map of the mean dimension [mm] of the 1-ring neighbourhood.

Test case	AQ method			Pan and Wu method			
	$\varphi$ [°]	d [mm]	t [s]	$\varphi$ [°]	d [mm]	t [s]	
1	$AF_0$	2.67	0.01	125.2	4.57	2.86	187.0
	$AF_{+20}$	1.90	0.15	120.4	1.97	25.25	526.2
	$AF_{+40}$	4.09	0.05	340.3	6.68	33.4	819.5
	$AF_{-20}$	2.39	0.1	124.7	11.10	5.76	108.4
	$AF_{-40}$	3.34	1.8	142.3	12.22	9.8	522.2
9	$AF_0$	2.21	0.01	142.6	7.73	0.61	198.6
	$AF_{+20}$	3.63	0.02	119.2	7.14	4.23	130.9
	$AF_{+40}$	6.74	0.01	418.7	7.66	29.73	1293.3
	$AF_{-20}$	2.39	0.16	135.6	6.82	6.52	562.8
	$AF_{-40}$	6.21	0.14	513.3	18.10	27.34	951.4

Tab. 1: Results regarding robustness against asymmetrically scanned faces.

			$AF_0$	$AF_{+20}$	$AF_{+40}$	$AF_{-20}$	$AF_{-40}$
<i>AQ method</i>	$\varphi$ [°]	Mean	2,24	3,40	4,65	4,64	4,34
		Max	4,30	8,01	6,74	8,22	8,85
		std	1,28	2,11	2,01	2,85	2,44
	d [mm]	Mean	0,04	0,07	0,10	0,08	0,57
		Max	0,10	0,16	0,18	0,16	1,80
		std	0,04	0,06	0,07	0,05	0,71
	t [s]	Mean	97,0	82,1	186,5	122,9	180,6
		Max	183,2	239,0	418,7	240,1	513,3
		std	66,1	83,3	137,9	65,2	148,5
<i>Pan and Wu method</i>	$\varphi$ [°]	Mean	15,00	17,50	40,45	24,59	47,02
		Max	35,68	35,07	88,27	39,42	86,10
		std	12,32	7,82	29,73	12,66	26,01
	d [mm]	Mean	3,64	10,04	17,15	14,41	28,31
		Max	10,39	18,03	30,35	22,10	41,34
		std	3,22	4,61	7,91	6,18	6,22
	t [s]	Mean	82,5	103,4	111,4	198,2	191,9
		Max	125,8	208,5	191,2	467,4	471,5
		std	25,5	54,4	53,0	141,3	156,6

Tab. 2: Results regarding the errors of the two methods.

The experiment is carried out in order to verify how the asymmetrically scanned data affect the estimation of the *symmetry plane* in the two methods which are here analysed. This is investigated by analysing 5 different acquisitions of the face of 15 test people maintaining the same neutral facial expression and closed eyes. The 5 different acquisitions are obtained by scanning the same faces from different angles of view ( $-40^\circ$ ,  $-20^\circ$ ,  $0^\circ$ ,  $20^\circ$ ,  $40^\circ$ ). Figure 3 shows a schematic representation (not to scale) of the different positions assumed by the optical scanner with respect to the sagittal plane of the subject's face. The labels of the different acquisitions are reported in the same figure.

In order to evaluate the performance of the two methods, each acquisition is compared with a reference face (*RF*). The *RF* is constructed by registering different acquisitions from different angles of view so that the whole face is obtained. The obtained point cloud is decimated for the sampling density to be uniform all over the face. In this way the reference face is not affected by asymmetries coming from the sampling and acquisition process. The *symmetry plane* of the  $RF(\Pi_{RF})$  has been estimated by using the two methods here compared. Results are substantially identical (the angle between the planes' normal unit vectors being  $<2.0^\circ$ ). It seems evident therefore that both methods work the same when input data are symmetrical.

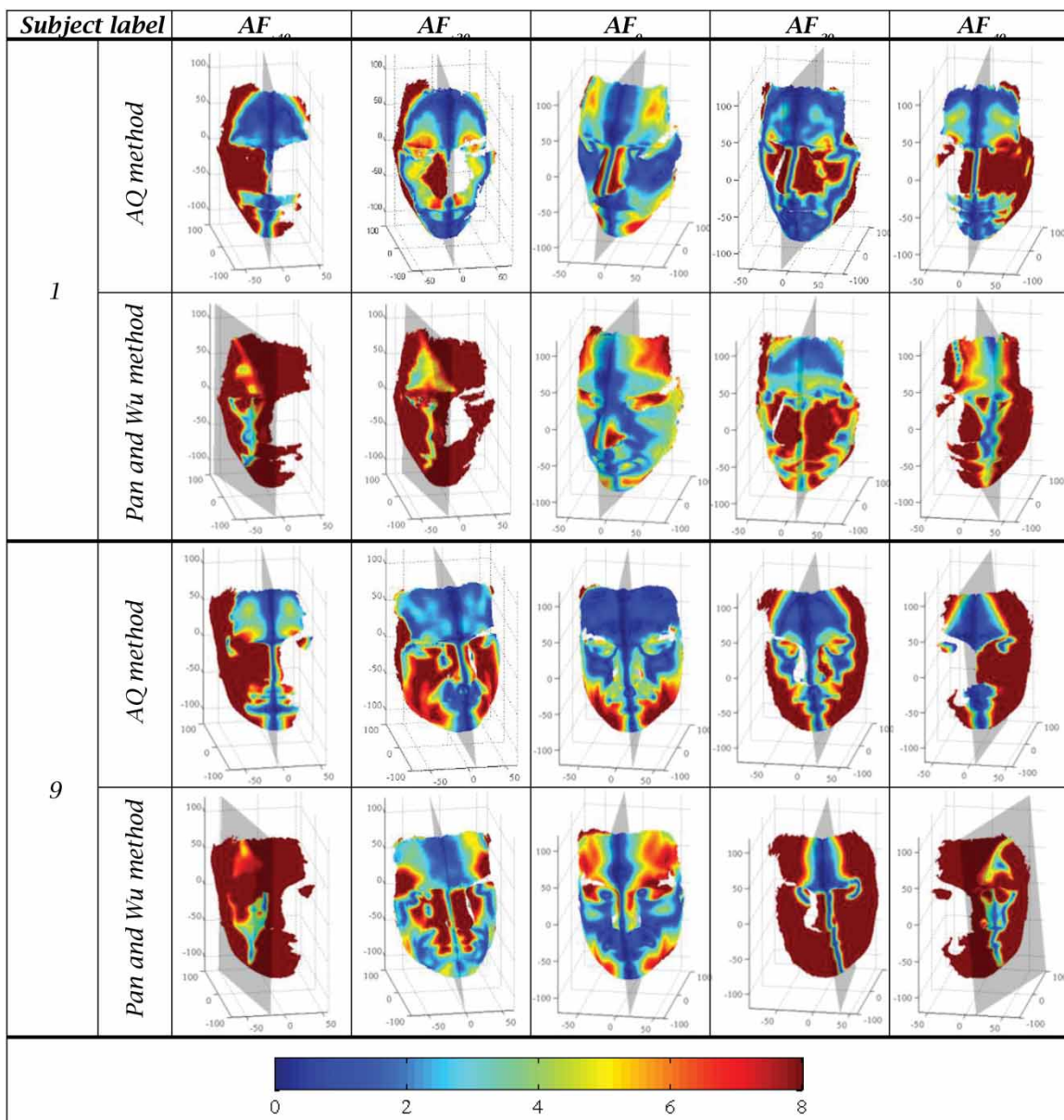


Fig. 6: Map of the Hausdorff distance [mm] and symmetry plane for the test cases of Figure 3.

Each of the 5 different acquisitions ( $AF_{-40}$ ,  $AF_{-20}$ ,  $AF_0$ ,  $AF_{+20}$ ,  $AF_{+40}$ ) is registered at the  $RF$  by means of the  $ICP$  algorithm of the methods being compared (namely, the  $AQ$  and  $Pan$  and  $Wu$  methods). Then the *symmetry plane* of each registered face ( $\Pi_{AF_{-40}}$ ,  $\Pi_{AF_{-20}}$ ,  $\Pi_{AF_0}$ ,  $\Pi_{AF_{+20}}$ ,  $\Pi_{AF_{+40}}$ ) is estimated and any difference from  $\Pi_{RF}$  is measured as the distance ( $d$ ) with respect to  $\Pi_{RF}$  and the angle between the related normal unit vectors:

$$\varphi_i = \arccos(\mathbf{n}_r \cdot \mathbf{n}_{i,reg}) \quad (4.1)$$

where  $\mathbf{n}_r$  and  $\mathbf{n}_{i,reg}$  are, respectively, the normal unit vector of the *symmetry plane* of the reference face and the normal unit vector of the *symmetry plane* of the  $i$ -th face, expressed in the coordinate system of the reference face.

In figure 4 two of the 15 test cases analysed are depicted. In this figure, the asymmetries in the sampled face area are evident.

The sampling dimension of two acquisitions is mapped in figure 5. The difference of density sampling due to the surface normal orientation with respect to the observation direction is remarkable. Analogous results can be observed in all the acquired faces.

Table 1 reports the results for the comparison of the two test cases depicted in figure 4. It seems evident that the  $AQ$  method recognises the *symmetry plane* better than the  $Pan$  and  $Wu$  method. The greatest angular error performed by the  $AQ$  method is  $6.74^\circ$  whereas for the  $Pan$  and  $Wu$  method it is  $18.10^\circ$ .

For each acquisition the *Hausdorff distance* has been calculated between the  $AF_i$  and its mirroring image which has been obtained by its estimated *symmetry plane*. In figure 6 the maps of the *Hausdorff distance* are depicted for the two test cases of figure 4.

The maps show a good performance of the  $AQ$  method even in the most extreme conditions. On the contrary, the  $Wu$  and  $Pan$  method yields very poor results.

Finally, table 2 summarises the results obtained for the all the 15 test cases analysed. As regards the method here proposed, the *symmetry plane* error measured by  $\varphi$  and  $d$  increases slightly with the angle between the observation direction and the sagittal plane of the face. The asymmetries in the scanned data affect greatly the computing time of the  $AQ$  method. Indeed, the method's iterations of the  $ICP$  registration process increase in those cases. Evidence is shown in the data in table 2.

## 5. CONCLUSIONS

As evidenced by the experiments explained in this paper, even the most promising method presented in literature falls short when it comes to estimating the *symmetry plane* of an asymmetrically scanned human face. Such is the case of the  $Pan$  and  $Wu$  method [14], which has been implemented by these authors for

the sake of comparison with the new method being presented.

The proposed method is specifically designed to process a face acquired with a single scanning session and which, for this very reason, is incomplete, asymmetrically scanned and non-uniformly sampled. This method is validated by analysing 5 different acquisitions, obtained from different angles of view, of the face of 15 people which maintain the same neutral facial expression and closed eyes. The results obtained show that the proposed method is practically insensitive both to asymmetrically scanned data and to non-uniformity in point cloud density. It proves to be a good tool for all those practical applications where the human face is acquired quickly and incompletely. Typical applications could be face authentication and recognition as well as clinical investigation. The performances is limited by necessity of disposing of high density point cloud; this requires heavy computational resources.

## REFERENCES

- [1] Barone, S.; Paoli, A.; Rationale, A.V.: Multiple alignments of range maps by active stereo imaging and global marker framing, *Optics and Lasers in Engineering*, 51(2), 2013, 116-127, <http://dx.doi.org/10.1016/j.optlaseng.2012.09.003>.
- [2] Benz, M.; Laboureux, X.; Maier, T.; Nkenke, E.; Seeger, S.; Neukam, F.-W.; Häusler, G.: The symmetry of faces, *Proceedings of VMV'2002*. Erlangen, Germany.
- [3] Besl, P.-J.; McKay, N.-D.: A method for registration of 3D shapes, *IEEE Transactions on Pattern Analysis and Machine Intelligence*, 14(2), 1992, 239-256, <http://dx.doi.org/10.1109/34.121791>.
- [4] Black, M.-J.; Rangarajan, A.: On the unification of line processes, outlier rejection, and robust statistics, *International Journal of Computer Vision*, 19 (1), 1996, 57-91, <http://dx.doi.org/10.1007/BF00131148>.
- [5] Colbry, D.; Stockman, G.: Canonical face depth map: A robust 3d representation for face verification, In *CVPR '07: Proceedings of the 2007 IEEE Computer Society Conference on Computer Vision and Pattern Recognition (CVPR'07)*, Minneapolis, MN, USA, 2007, 1-7, <http://dx.doi.org/10.1109/CVPR.2007.383108>.
- [6] Combès, B.; Hennessy, R.; Waddington, J.; N. Roberts, S. Prima. An algorithm to map asymmetries of bilateral objects in point clouds, *International Symposium on Biomedical Imaging: From Nano to Macro*, Paris, France, 2008, <http://dx.doi.org/10.1109/ISBI.2008.4541202>.
- [7] Combès, B.; Hennessy, R.; Waddington, J.; Roberts, N.; Prima, S.: Automatic symmetry plane estimation of bilateral objects in point clouds, *International conference on computer*



- vision and pattern recognition 2008, Anchorage, United States, 2008, <http://dx.doi.org/10.1109/CVPR.2008.4587605>.
- [8] Combès, B.; Prima, S.: New algorithms to map asymmetries of 3D surfaces, International Conference on Medical Image Computing and Computer Assisted Intervention, 2008, [http://dx.doi.org/10.1007/978-3-540-85988-8\\_3](http://dx.doi.org/10.1007/978-3-540-85988-8_3).
- [9] De Momi, E.; Chapuis, J.; Pappas, I.; Ferrigno, G.; Hallermann, W.; Schramm, A.; Caversaccio, M.: Automatic extraction of the mid-facial plane for craniomaxillofacial surgery planning, The International Journal of Oral & Maxillofacial Surgery, 35(7), 2006, 636-642, <http://dx.doi.org/10.1016/j.ijom.2006.01.028>.
- [10] Hennessy, R.-J.; McLearn, S.; Kinsella, K.; Waddington, J.-L.: Facial shape and asymmetry by three dimensional laser surface scanning covary with cognition in a sexually dimorphic manner, The Journal of Neuropsychiatry and Clinical Neurosciences, 18(1), 2006, 73-80, <http://dx.doi.org/10.1176/appi.neuropsych.18.1.73>.
- [11] Ikemitsu, H.; Zeze, R.; Yuasa, K.; Izumi, K.: The relationship between jaw deformity and scoliosis, Oral Radiology, 22(1), 2006, 14-17, <http://dx.doi.org/10.1007/s11282-006-0039-6>.
- [12] Pan, G.; Wang, Y.; Qi, Y.; Wu, Z.: Finding symmetry plane of 3D face shape. International Conference on Pattern Recognition, 3, 2006, 1143-1146, <http://dx.doi.org/10.1109/ICPR.2006.565>.
- [13] Pan, G.; Wu, Z.: 3d face recognition from range data, International Journal of Image and Graphics, 5(3), 2005, 1-21, <http://dx.doi.org/10.1142/S0219467805001884>.
- [14] Pearson, K.: On lines and planes of closest fit to systems of points in space, Philosophical Magazine 2 (6), 1901, 559-572, <http://dx.doi.org/10.1080/14786440109462720>.
- [15] Rusinkiewicz, S.; Hall-Holt, O.; Levoy, M.: Real-time 3D model acquisition, Computer Graphics Proceedings SIGGRAPH 2002, 438-446, <http://dx.doi.org/10.1145/566570.566600>.
- [16] Seeger, S.; Laboureux, X.; Häusler, G.: An accelerated ICP - algorithm, Lehrstuhl für Optik, Annual Report, Erlangen, (2001).
- [17] Spreeuwers, L.: Fast and Accurate 3D Face Recognition, International Journal of Computer Vision, 93 (3), 2011, 389-414, <http://dx.doi.org/10.1007/s11263-011-0426-2>.
- [18] Sun, C.; Sherrah, J.: 3d symmetry detection using the extended Gaussian image, IEEE transactions on pattern analysis and machine intelligence, 19(2), 1997, 164-168, <http://dx.doi.org/10.1109/34.574800>.
- [19] Surazhsky, T.; Magid, E.; Soldea, O.; Elber, G.; Rivlin, E.: A comparison of Gaussian and mean curvatures estimation methods on triangular meshes, IEEE ICRA'03, 2003, 1021-1026, <http://dx.doi.org/10.1109/ROBOT.2003.1241726>.
- [20] Tang, X.-M.; Chen, J.-S.; Moon Y. S.: Accurate 3d face registration based on the symmetry plane analysis on nose regions, 16th European Signal Processing Conference (EUSIPCO 2008), Lausanne, Switzerland, August 25-29, 2008,
- [21] Zhang, L.; Razdan, A.; Farin, G.; Bae, M.-S.; Femiani, J.: 3d face authentication and recognition based in bilateral symmetry analysis, Journal of Visual Computer, 22(1), 2006, 43-55, <http://dx.doi.org/10.1007/s00371-005-0352-9>.